

STUDY ON ENHANCEMENT AND WEAKENING OF PERMANENT MAGNET AIR-GAP FLUX DENSITY

J. S. Hsu
Oak Ridge National Laboratory
2360 Cherahala Boulevard
Knoxville, Tennessee 37932, U.S.A.

Abstract—In a conventional permanent magnet (PM) machine, the air-gap flux produced by the PMs is fixed. It is difficult to enhance the air-gap flux density because of limitations of the PMs in a series magnetic circuit. However, the air-gap flux density can be weakened by using power electronics to weaken the field, up to the limit of demagnetization of the PMs. This paper presents an analytical study for controlling the PM air-gap flux density through a stationary brushless excitation coil. The air-gap flux density can be either enhanced or weakened. There is no concern with demagnetizing the PMs during field weakening. The leakage flux of the excitation coil through the PMs is blocked. The prototype motors built on this principle confirm the concept and verify the capability to significantly flux enhance and weaken the magnetic field

STUDY ON ENHANCEMENT AND WEAKENING OF PERMANENT MAGNET AIR-GAP FLUX DENSITY*

I. INTRODUCTION

For electric vehicle (EV) and hybrid-electric vehicle (HEV) drive systems, a high torque is needed to start and accelerate the vehicle. After the base speed is reached, the required torque gradually diminishes and the speed goes up in a constant power mode. A constant power speed ratio (CPSR) is the ratio of the highest possible speed delivering the base power to the base speed. For a given maximum current, the motor torque is proportional to the flux; any additional torque in the start-up and acceleration regions requires that the motor flux be increased. Therefore, field enhancement is desirable. Above base speed, the motor flux needs to be weakened which reduces the induced back-electromotive force (emf) voltage to allow a higher current for producing a high CPSR. Some additional background information is given in Refs. [1–7].

A power electronic inverter can provide field weakening up to the limit where it causes demagnetization of the permanent magnets (PMs). Field enhancement does not increase conventional PM motor performance owing to saturation of the PMs. This paper presents an analytical study showing that by controlling the current of a stationary brushless coil, the air-gap flux can be enhanced without being limited by PM saturation and that the air-gap flux density can also be weakened. The flux diffusion (or leakage) in the magnetic path from the excitation coil to the rotor poles can be blocked by using PMs.

A description of the high-strength undiffused brushless motors built on the principle of this analytical study is submitted in this paper.

II. PM AIR-GAP FLUX DENSITY OF SIMPLE MAGNETIC CIRCUIT

A simple PM magnetic circuit that has the PM connected in series with the air gaps and the return magnetic core is shown in Fig. 1. B represents flux density; H , magnetic field strength; L , length; A , area; and I , current. The suffix g stands for the air gap, pm for PM, and a for armature (for example, B_g represents the air-gap flux density). This circuit represents a conventional PM motor that has a pair of air gaps between the PM and the stator core and an armature winding with current I_a . A positive current direction shown in Fig. 1 produces a positive field in the direction shown for B and H .

* Research sponsored by the Oak Ridge National Laboratory managed by UT-Battelle, LLC, for the U. S. Department of Energy under contract DE-AC05-00OR22725.

The submitted manuscript has been authored by a contractor of the U. S. Government under contract No. DE-AC05-00OR22725. Accordingly, the U. S. Government retains a nonexclusive, royalty-free license to publish or reproduce the published form of this contribution, or allow others to do so, for U. S. Government purposes.

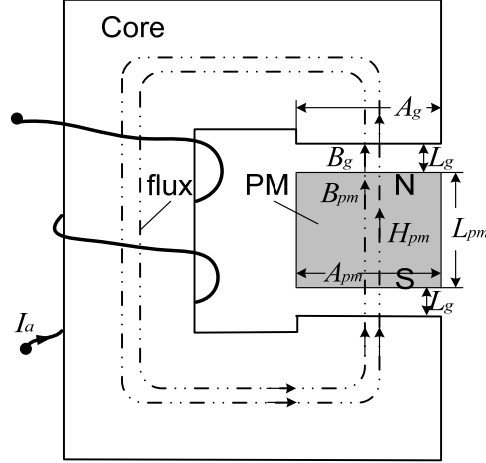


Fig. 1. A simple series magnetic circuit.

Electromagnetic circuit theory is based on two fundamental laws [8]. The first law (Ampere's law) is "The line integral of the magnetic field strength or intensity taken around any closed path is proportional to the total current flowing across any area bounded by that path." In symbols, the first law is

$$\oint H \cdot dL = \sum I . \quad (1)$$

Applying Eq. (1) to the simple series magnetic circuit shown in Fig. 1 gives

$$H_{pm} \cdot L_{pm} + 2 \cdot \frac{B_g}{\mu_0} \cdot L_g = \sum I_a , \quad (2)$$

where μ_0 is the permeability in air and $\sum I_a$ is the product of the number of turns and the current I_a . The right-hand rule is used to determine the sign of the field produced by $\sum I_a$. In Eq. (2) it is assumed that the core magnetic saturation is negligible. Because the flux must be continuous, if we ignore the leakage flux and assume the PM area A_{pm} is the same as the air gap area A_g , we have

$$B_g = B_{pm} . \quad (3)$$

Substituting Eq. (3) into Eq. (2) gives

$$B_g = B_{pm} = \left(\frac{\sum I_a}{L_{pm}} - H_{pm} \right) \cdot \left(\frac{L_{pm}}{2 \cdot L_g} \right) \cdot \mu_0 . \quad (4)$$

The intrinsic-flux density [9] is the contribution of the magnetic material to the total magnetic-flux density (B). It is the vector difference between the total magnetic-flux density in the material and the magnetic-flux density that would exist in a vacuum under the same field strength (H). This relation is expressed by subtracting the magnetic-flux density produced by H in a vacuum from the value of B .

Substituting Eq. (4) into the definition of intrinsic-flux density gives

$$B_{pm} - H_{pm} \cdot \mu_0 = \left(\frac{\sum I_a}{L_{pm} + 2 \cdot L_g} - H_{pm} \right) \cdot \left(\frac{L_{pm}}{2 \cdot L_g} + 1 \right) \cdot \mu_0. \quad (5)$$

Figure 2 shows the familiar graphical approaches for obtaining the air-gap flux density B_g through either the actual demagnetization B/H curve or the intrinsic induction B/H curve. The slopes, $\left(\frac{L_{pm}}{2 \cdot L_g} \right) \cdot \mu_0$ and $\left(\frac{L_{pm}}{2 \cdot L_g} + 1 \right) \cdot \mu_0$, of the permeance coefficient lines used for intersecting the B/H curves are different in both cases, as indicated in Eqs. (4) and (5). Either approach gives the same air-gap flux density B_g . Figure 2 also includes a small demagnetization current (i.e., I_a is negative) from the armature reaction. The starting points a and a' for the methods using the actual demagnetization B/H curve and using the intrinsic induction B/H curve, respectively, are very close to each other. One is located at $\frac{\sum I_a}{L_{pm}}$ and the other one at $\frac{\sum I_a}{L_{pm} + 2 \cdot L_g}$.

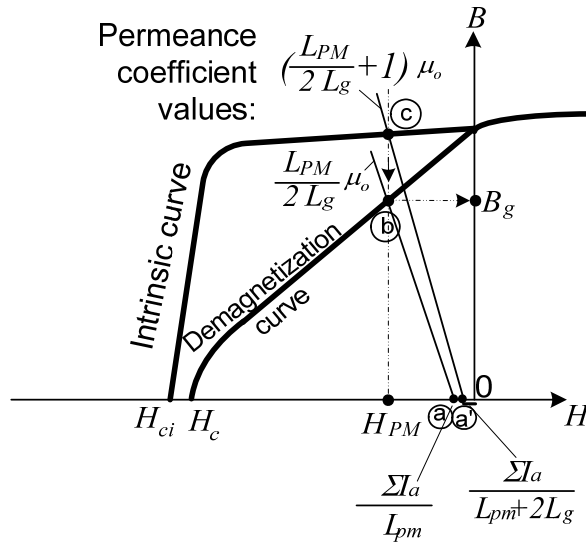


Fig. 2. Familiar graphical approaches for obtaining air-gap flux density.

The demagnetization caused by the value of the negative $\sum I_a$ divided by the PM thickness L_{pm} or by $(L_{pm} + 2 \cdot L_g)$ suggests that a thicker PM can prevent permanent damage to the PM from the demagnetizing armature reaction.

Figure 3 shows that when the armature current I_a is a positive value, point a or a' is in the positive direction of the horizontal coordinate. This causes the air-gap flux density B_g to rise. However, the field enhancement is limited by the saturation of the PM B/H curve because the air-gap flux density can never be higher than the PM flux density.

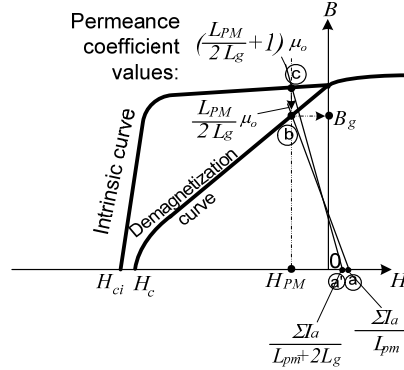


Fig. 3. Air-gap flux density with field enhancement of a conventional PM machine.

III. MAGNETIC EQUATIONS FOR SYSTEM EXCITED BY PM AND FIELD CURRENT

Figure 4 shows the magnetic paths for a system excited by both PM and field current $\sum I_f$, with the armature reaction $\sum I_a$ taken into consideration. For simplicity, the components of the magnetic circuit shown in Fig. 4 are in a uniform thickness. The upper and lower dimensions are symmetrical. The left-side gaps are defined as the main air gaps L_{g1} and the right-side gaps are defined as the excitation gaps L_{g2} . The same nomenclature mentioned earlier applies to this analysis.

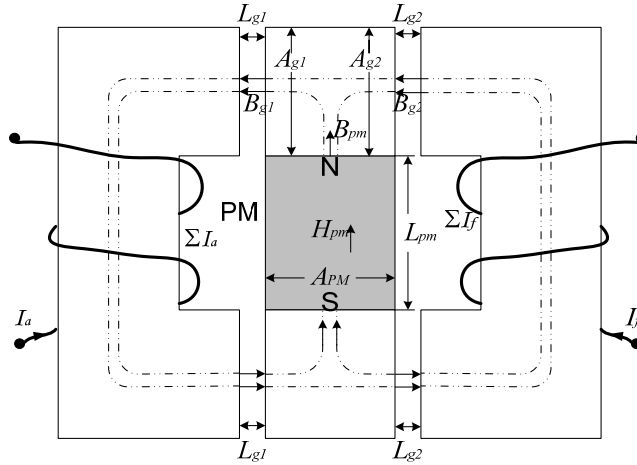


Fig. 4. Magnetic paths for system excited by both PM and field current with armature reaction.

An examination of the center upper core reveals that, because the magnetic flux must be continuous, the total flux going into the core is zero;

$$B_{g1} \cdot A_{g1} = B_{g2} \cdot A_{g2} + B_{pm} \cdot A_{pm}, \quad (6)$$

where the symbol B represents flux density, A is for area, and g is the air gap. The suffix $g1$ is for the left-side main air gap; $g2$, the right-side excitation air gap; and pm , the PM.

For the magnetic path that goes through the gaps, the equation, according to the first law Eq. (1) is

$$\sum I_f + \sum I_a = 2 \cdot \frac{B_{g2}}{\mu_0} \cdot L_{g2} + 2 \cdot \frac{B_{g1}}{\mu_0} \cdot L_{g1}, \quad (7)$$

where the air-gap permeability μ_0 is used to relate B_{g1} and B_{g2} to H_{g1} and H_{g2} , respectively.

For the right half magnetic circuit we have

$$\sum I_f = 2 \cdot \frac{B_{g2}}{\mu_0} \cdot L_{g2} - H_{pm} \cdot L_{pm}. \quad (8)$$

For the left half magnetic circuit, we have

$$\sum I_a = 2 \cdot \frac{B_{g1}}{\mu_0} \cdot L_{g1} + H_{pm} \cdot L_{pm}. \quad (9)$$

Adding Eqs. (7) and (8) yields

$$2 \cdot \sum I_f + \sum I_a = -H_{pm} \cdot L_{pm} + 4 \cdot \frac{B_{g2}}{\mu_0} \cdot L_{g2} + 2 \cdot \frac{B_{g1}}{\mu_0} \cdot L_{g1}. \quad (10)$$

Substituting B_{g2} from Eq. (6) to Eq. (10)

$$2 \cdot \sum I_f + \sum I_a = -H_{pm} \cdot L_{pm} - 4 \cdot \frac{L_{g2}}{\mu_0} \cdot \frac{A_{pm}}{A_{g2}} \cdot B_{pm} + \left(4 \cdot \frac{L_{g2}}{\mu_0} \cdot \frac{A_{g1}}{A_{g2}} + 2 \cdot \frac{L_{g1}}{\mu_0} \right) \cdot B_{g1}. \quad (11)$$

Substituting B_{g1} from Eq. (9) to Eq. (11)

$$B_{PM} + \frac{A_{g1} \cdot L_{pm} \cdot \mu_0}{A_{pm} \cdot 2 \cdot L_{g1}} \cdot H_{pm} = \frac{A_{g2} \cdot L_{pm} \cdot \mu_0}{A_{pm} \cdot 2 \cdot L_{g2}} \cdot \left(\frac{-\sum I_f + \frac{A_{g1} \cdot L_{g2}}{A_{g2} \cdot L_{g1}} \sum I_a}{L_{pm}} - H_{pm} \right). \quad (12)$$

The relationship between the main air-gap flux density B_{g1} and the PM field strength H_{PM} can be derived from Eq. (9) as

$$B_{g1} = \left(\frac{\sum I_a}{L_{pm}} - H_{pm} \right) \cdot \left(\frac{L_{pm}}{2 \cdot L_{g1}} \cdot \mu_0 \right). \quad (13)$$

$$\left(\frac{-\sum I_f + \frac{A_{g1} \cdot L_{g2}}{A_{g2} \cdot L_{g1}} \sum I_a}{L_{pm}} - H_{pm} \right)$$

shown in the right side of Eq. (12) has a smaller magnitude than H_{pm} . A permeance coefficient line is drawn from point a and intercepts the curve that represents the left portion of Eq. (12). A vertical line is then drawn from point b and intercepts the horizontal coordinate at point c for the H_{pm} value. This H_{pm} value is the graphical solution of Eq. (12) at point b. The vertical line from point b can be further extended upward to intercept the demagnetization curve for the flux density B_{PM} in the PM and to intercept the permeance coefficient line defined by Eq. (13) for the main air-gap flux density B_{g1} . Unlike in the conventional PM machine, the value of B_{g1} is not limited by the PM flux density. It can be higher than the PM flux density. In practice, the degree of enhancement is limited by the core material saturation level, which is normally higher than that of the PM, and by the requirement that the value of

$$\frac{-\sum I_f + \frac{A_{g1} \cdot L_{g2}}{A_{g2} \cdot L_{g1}} \sum I_a}{L_{pm}}$$

not reach the demagnetization level. When a thicker PM is used, the slope of the operating line increases and its intercept moves closer to the origin so that the permanent demagnetization of the PM should not be a concern. Another property of this magnetic circuit is that since the PM flux opposes the field excitation during field enhancement, the leakage (or diffusion) flux of the excitation coil is blocked by the PMs.

Figure 6 shows the graphical solution for the field weakening case in the main air gap L_{g1} . Reversing the direction of a sufficiently high field current, I_f , causes point a to move to the right. The air-gap flux density B_{g1} and the PM flux density B_{pm} can be obtained. The PM would never be demagnetized under the field weakening situation for this magnetic circuit. The air-gap flux density B_{g1} is significantly reduced, as the PM flux is diverted through L_{g2} .

When the demagnetization curves are plotted with Gauss and Oersted as the units for the vertical and horizontal coordinates, respectively, the μ_0 can be omitted, as μ_0 equals Gauss/Oersted.

REFERENCES

- [1] J. S. Hsu, "Hybrid-Secondary Uncluttered Induction (HSU-I) Machine," *PES/IEEE Transactions on Energy Conversions*, Paper No. PE-259EC, February 2001.
- [2] J. S. Hsu, *Hybrid Secondary Uncluttered Induction Machine*, U.S. Patent No. 6,310,417, October 30, 2001.
- [3] J. S. Hsu, "Direct Control of Air Gap Flux in Permanent-Magnet Machines," pp. 361–365 in *PES/IEEE Transactions on Energy Conversions*, **15**(4), December 2000.
- [4] T. Mizuno, K. Nagayama, T. Ashikaga, and T. Kobayashi, "Basic Principles and Characteristics of Hybrid Excitation Synchronous Machine," pp. 1402–1411 in *Electrical Engineering in Japan*, **117**(5), 1996; translated from *Denki Gakkai Ronbunshi*, **115-D**(11), November 1995.
- [5] J. S. Hsu, *Direct Control of Air Gap Flux in Permanent-Magnet Machines*, U.S. Patent No. 6,057,622, May 2, 2000.
- [6] J. S. Hsu, "Flux Guides for Permanent-Magnet Machines," *PES/IEEE Transactions on Energy Conversions*, Paper No. PE-007EC, March 2001.
- [7] J. S. Hsu, *High Strength Undiffused Brushless Machines*, U.S. Patent No. 6,573,634, June 3, 2003.
- [8] D. G. Fink and J. M. Carroll, *Standard Handbook for Electrical Engineers*, 10th edition, McGraw-Hill Book Company, 1969.
- [9] J. H. Ireland, *Ceramic Permanent-Magnet Motors*, McGraw-Hill Book Company, 1968.